JOURNAL OF GEOPHYSICAL RESEARCH, VOL. 96, NO. B4, PAGES 6779–6796, APRIL 10, 1991

Influence of Glacial Isostatic Adjustment on Tide Gauge Measurements of Secular Sea Level Change

W. R. PELTIER AND A.M. TUSHINGHAM

Department of Physics, University of Toronto, Toronto, Ontario, Canada

Modern tide gage records of secular sea level change are strongly contaminated by the ongoing influence of glacial isostatic adjustment. In this paper we employ an accurate high- resolution model of the glacial isostatic adjustment process to filter this signal from time series consisting of annual mean heights observed on over 500 tide gages from which records of duration longer than 10 years are available. These records are all contained in the archive of the Permanent Service for Mean Sea Level at Bidston in the United Kingdom. Prior to removal of the isostatic adjustment contamination from these records the secular sea level change signal is seen to exhibit both rising and falling levels depending upon geographic location, with regions of falling level corresponding to those that were ice covered during the last glaciation event of the present ice age. After filtering, the geographic heterogeneity in rates is considerably reduced, so much so that a globally coherent component consisting of a rise of sea level at a rate of 2.4 ± 0.9 mm yr^{-1} is revealed. This could conceivably be driven by the "greenhouse effect," although no particular mechanism has been unambiguously identified by our analyses. We investigate the impact of a number of different variants of the analysis procedure upon the inferred global signal.

INTRODUCTION

Secular variations of sea level determined by monthly or annually averaged tide gauge observations have often been employed as possible indicators of climatic change, due either to cyclical affects or to "greenhouse" warming [e.g., *Gutenberg*, 1941; *Hicks*, 1978; *Gornitz et al.*, 1982; *Barnett*, 1983]. On the basis of such analyses, particularly those of *Barnett* [1983, 1984], it has been suggested that sea level has apparently risen by 10-20 cm since 1900. Because of the extreme geographic heterogeneity in the rates, however, and the poor coverage of the southern oceans by gages of reasonable seniority, it has not been possible to argue convincingly that any globally coherent signal of secular sea level rise was active in the system such as might be caused by "greenhouse" warming. There is also considerable ongoing controversy on the question as to what fraction of the sea level signal might be explicable in terms of the steric effect of thermal expansion of the oceans rather than requiring an increase in the actual mass of water in the ocean basins [e.g., *Gornitz et al.*, 1982; *Roemmich and Wunsch*, 1984; *Roemmich*, 1985]. Based upon these analyses it would appear that no more than about 5 cm of the global sea level rise since 1900 could be of steric origin, and this amount would be considered an upper bound by most oceanographers. The remaining (and dominant) contribution to the signal clearly requires that the mass of water in the oceans be increasing, and the precise source of this water remains illusive. *Meier* [1984] has shown that somewhat less than 5 cm might be explicable as an effect due to the melting of the small ice sheets and glaciers of the world, systems whose mass balances are reasonably well constrained by direct measurements over the past century. Any deficit between the sum of the steric and small glaciers contributions and the tide gage constraint would most probably have to be made up by mass loss from the large ice sheets on Greenland and Antarctica, systems whose balances are relatively poorly constrained.

Our intention in the present paper is to present further analyses that we have performed in an effort to better constrain the nature of the global signal that the tide gages reveal. A great many different mechanisms do in fact clearly contribute to the variations of relative sea level that are recorded on an individual tide gage and in their totality serve to mask any globally coherent signal that might be associated with climatic warming. These have been reviewed, for example, by *Fairbridge and Krebs* [1962] and *Aubrey and Emery* [1988] and would include (1) relative sea level (RSL) variations due to long time scale changes in the onshore component of wind stress, (2) RSL variations caused by river runoff effects associated with changes in precipitation in the controlling watershed, (3) RSL variations caused by changes in the hydraulic head effect operating in narrow straights such as the Florida straights or the Skagerak (between Denmark and Norway), (4) RSL variations associated with steric (density) changes due to alterations of temperature or salinity, and (5) RSL variations caused by geological processes involving the solid earth such as sedimentary loading in river deltas like the Mississippi and the Nile and tectonic effects. If we could accurately remove all of these contributions to every tide gage record, we would clearly be able to estimate much more accurately the secular component of change that is of such interest from a climatological point of view. Our focus in this paper will be on the impact which the removal of one such source of variability, namely, the influence of the glacial isostatic adjustment process, has upon our ability to estimate the secular component of RSL change that could be due to global climate warming. As we will show, this single process

Paper number 90JB02067.
0148-0227/91/90JB-02067$05.00

constitutes a bias on the tide gage records that substantially reduces the rate of RSL rise inferred from the observations and contributes significantly to its geographic variability. Correcting the data for this effect therefore yields an estimate for the global rate of RSL rise that is significantly higher and, as we will show, significantly more spatially coherent than previous estimates.

That the influence of glacial isostatic adjustment does constitute a significant source of contamination on tide gage measurements of secular sea level change is an idea that has been developed in a number of recent articles. *Peltier* [1986] conducted an initial assessment of this influence that focused on tide gage records from the North American continent, especially on those from the heavily instrumented east coast of the United States. Because this region lies entirely within the zone of forebulge collapse [e.g., *Peltier*, 1974] peripheral to the location of the Laurentide (Canadian) ice sheet at glacial maximum, sea levels continue to rise along this coast due in part to this cause. However, when the data were corrected for this effect, an effect which amounted to as much as 2 mm yr^{-1} of RSL rise at some sites, a significant residual was found to remain. The residual was computed to be, on average, between 1.5 and 2 mm yr^{-1} and therefore close to the global estimate of the present day rate of RSL rise that had been inferred by *Barnett* [1983, 1984]. This suggested that the global influence of glacial isostatic adjustment on secular sea level change should be computed and employed to correct all of the tide gage data employed by Barnett. A preliminary map of this global signal was first published by *Peltier* [1988*a*]) wherein it was shown that even in the far field of the ice sheets, along the coastlines of South America and Africa, the isostatic adjustment contribution to the tide gage records amounted to a bias of between 0.4 and 0.6 mm yr^{-1} and the sense of this bias was that sea level was predicted to be falling so that correction for the bias would clearly lead to an increase in the secular rate of RSL rise inferred from the observations. A preliminary assessment of this global impact was presented by *Peltier and Tushingham* [1989], who employed both linear regression and empirical orthogonal function analysis to show that the decontaminated data revealed the presence of a global signal of strength 2.4 ± 0.9 mm yr^{-1} to be characteristic of a subset of the tide gauge records which they expected would be "optimal" for the extraction of any climatological contribution to RSL variability.

In the present paper we will expand considerably upon this preliminary analysis by investigating the sensitivity of this estimate to the manner in which the correction to the tide gage data for the influence of glacial isostatic adjustment is applied. This will allow us to assess better the robustness of the estimate and thus the extent to which it should be taken seriously as a constraint on scenarios of ongoing climatic change. The plan of the paper is as follows. In section 2 we will demonstrate the accuracy with which the radiocarbon record of long time scale RSL variability may be modeled using modern theories of the viscoelastic response of the Earth to deglaciation and will present the map of the present day rate of RSL change that has been delivered by the best available theory. In section 3 the tide gage data base employed for the analysis of secular sea level change is presented, and some comparisons are provided between the rates of RSL rise recorded in the data and the rates predicted by the model of glacial isostatic adjustment. Section 4 is concerned with the analysis of the tide gage data, both raw and isostatically reduced, using both the linear regression and empirical orthogonal function techniques. A large number of further variants on the analysis procedure will be therein discussed. Our main conclusions are summarized in section 5.

GLACIAL ISOSTATIC ADJUSTMENT AND RELATIVE SEA LEVEL CHANGE

Over the past 15 years, beginning with the paper by *Peltier* [1974], a detailed theory of the glacial isostatic adjustment process has been developed. This theory has been employed to reconcile a rather large collection of geophysical data, not only concerning postglacial relative sea level change [*Peltier and Andrews*, 1976; *Clark et al.*, 1978; *Wu and Peltier*, 1982; *Peltier*, 1984, 1986, 1988*b*] but also concerning the large-scale structure of the gravitational field [*Peltier*, 1981; *Peltier and Wu*, 1982; *Wu and Peltier*, 1983; *Mitrovica and Peltier*, 1989] and a number of previously unexplained anomalies in the Earth's rotational state [*Peltier*, 1982; *Wu and Peltier*, 1984; *Peltier*, 1985, 1988*a*]. Although it will serve no purpose in the present paper to review this theory in any detail, it will be useful to have before us a schematic representation of the mathematical relation that it delivers for the prediction of postglacial relative sea level change. If $S(\theta, \lambda, t)$ is the time dependent separation between the surface of the ocean (the geoid) and the surface of the solid earth at the point of their intersection with colatitude θ and east longitude λ, then the RSL history S is predicted by inverting the following integral equation:

$$S(\theta,\lambda,t) = \rho_I \frac{\phi}{g} * L_I + \rho_w \frac{\phi}{g} * S - \frac{1}{A_o} < \rho_I L_I * \frac{\phi}{g} + \rho_w S * \frac{\phi}{g} > o - \frac{M_I(t)}{\rho_w A_o} \quad (1)$$

in which ρ_I and ρ_w are the densities of ice and water, respectively, ϕ is the Green function for the perturbation of the gravitational potential field at the Earth's surface induced by a surface point load of 1 kg mass [*Peltier and Andrews*, 1976], g is the surface gravitational acceleration of the unperturbed spherical equilibrium configuration, A_o is the assume constant area of the Earth's oceans, the angle brackets indicate integration over the surface of the oceans, and $M_I(t)$ is the assumed known mass loss history of the ice sheets, one example of the form of which, expressed in terms of equivalent depth, is shown in Figure 1. In (1) the operation of

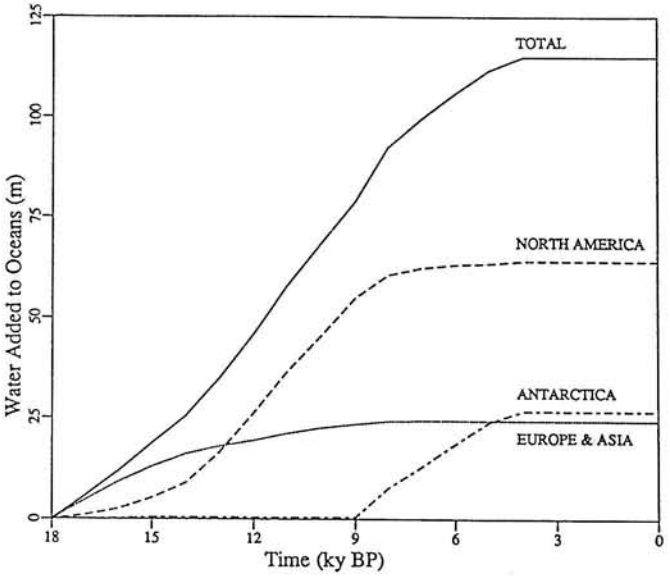

Fig. 1. Contributions to the global rise of sea level from both Northern and Southern Hemisphere ice complexes from the time of maximum Würm-Wisconsin glaciation at 18000 years before present until now.

space-time convolution is represented by the symbol asterisk. This equation is an integral equation because the unknown field $S(\theta, \lambda, t)$ appears both on the left-hand side and in the convolution operation on the right hand side. As discussed by *Peltier et al.* [1978], we solve it using an iterative scheme that starts with a eustatic first guess and uses the error to construct an improved solution, continuing until the equation is satisfied to within some prescribed tolerance.

Crucial to the implementation of this theory are an accurate model of the planetary deglaciation history $L_I(\theta, \lambda, t)$ and an accurate model for the internal radial viscoelastic structure of the planet that is required to determined the Green function ϕ. Since neither of these functionals of the model is perfectly determined on apriori grounds, the theory for postglacial sea level change embodied in (1) actually poses a nonlinear inverse problem for $L_I(\theta, \lambda, t)$ and for mantle viscosity $\nu(r)$ since the elastic part of the viscoelastic structure may be assumed to be determined by seismology. This inverse problem is solvable [*Peltier*, 1976; *Mitrovica and Peltier*, 1990] only because glacial geomorphological data may be invoked to deliver an apriori model for $L_I(\theta, \lambda, t)$. We proceed by first fixing L_I to this apriori determined field and vary $\nu(r)$ so as to achieve a best fit to the observations. We then fix $\nu(r)$ and perturb L_I away from the a priori estimate to improve the fit. This iterative process is continued until a best L_I and a best $\nu(r)$ are obtained. Objective methods are available with which one may converge to a solution and characterize its uniqueness [*Mitrovica and Peltier*, 1990]. For the purpose of the analyses to be presented in this paper we will employ the best currently available model of the deglaciation history that has been delivered by this process, namely, the ICE-3G model presented by *Tushingham and Peltier* [1990*b*]. The viscoelastic structure will also be fixed to that determined as best reconciling the totality of the previously enumerated geophysical constraints. This viscoelastic structure has an elastic component identical to model 1066B of *Gilbert and Dziewonski* [1975] and a viscous component that consists of an infinitely viscous near surface lithosphere of thickness 120 km, an upper mantle (between 120 km depth and the 670 km depth of the deepest seismic horizon) of viscosity 10^{21} Pa s, and a lower mantle (between 670 km depth and the core-mantle boundary) of viscosity 2×10^{21} Pa s.

In order to illustrate the quality of the fits to a newly constructed global compilation of ^{14}C-controlled RSL histories [*Tushingham and Peltier*, 1990*b*] that have been achieved with the theory embodied in (1), a sampling of comparisons will be presented here. In the interest of brevity this will be limited to a small number of locations from the complete set of approximately 400 sites shown on Figure 2. On this figure, locations marked as solid circles correspond to ice-covered sites from which ^{14}C-controlled RSL histories were employed in the refinement of the glaciation history. Sites marked as solid triangles were not employed to constrain the glaciation history and therefore may be legitimately employed for validation purposes. In Figures 3, 4, and 5 we present comparisons between observed RSL histories at 18 different locations and the predictions of the glacial isostatic adjustment model at these same locations. On each frame of these figures the corresponding data are compared to two different model predictions, one marked as a solid curve and the other as a dashed curve. These predictions respectively correspond to those made with the new ICE-3G model and those made using the previous ICE-2 model of *Wu and Peltier* [1983] which was of considerably lower resolution. Clearly the new high-resolution model has provided a vastly improved fit to the data, a goodness of fit which has been quantified in detail by *Tushingham and Peltier* [1990*b*].

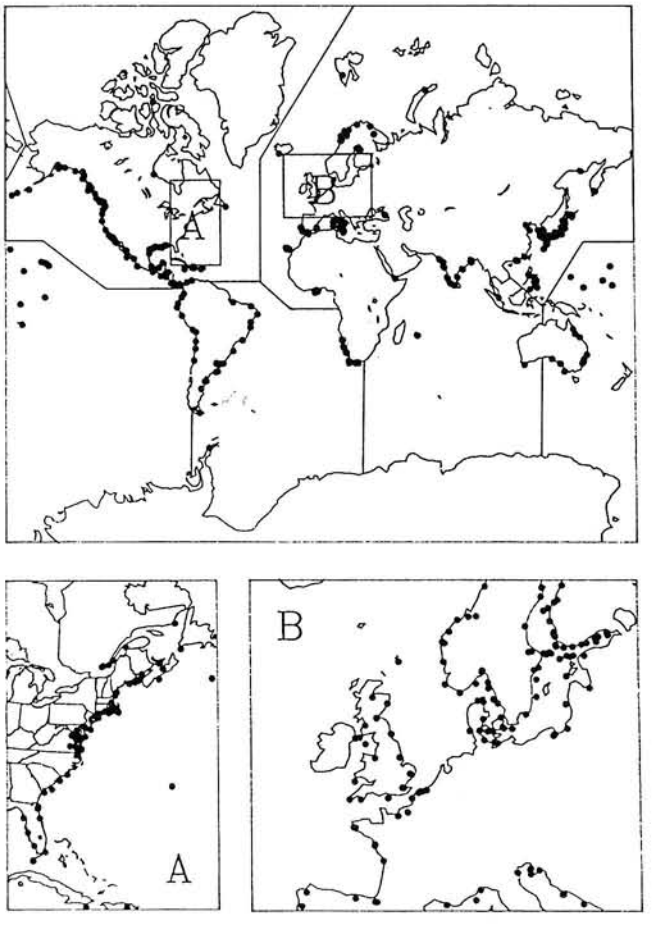

Fig. 2. Locations from which ^{14}C data on relative sea level history are available. The sites denoted as solid circles are those from which the RSL data were employed to constrain the melting chronology of the ice sites. Data from sites denoted by solid triangles were not employed in this adjustment process.

Given the very high quality fit to the global ^{14}C- controlled RSL data set that has been delivered by the isostatic adjustment model, it is clearly possible for us to use the model as a filter with which to remove this contribution to modern RSL variability from tide gage recordings. To this end we show in Plate 1 the present-day rate of secular sea level change that should be measured by a tide gage at every point on the Earth's surface if the only signal active in the system were that due to glacial isostatic adjustment. To compute this field, we have employed the high-resolution isostatic adjustment model and made predictions of RSL history on a fine spatial mesh with a sampling interval of 1 kyr from 18 ka until 1 kyr into the future. A centered finite difference was then employed to compute the present-day rate of RSL rise (fall) at each spatial point and the resultant map was color contoured on a high-resolution graphics display screen to produce Plate 1. The reader should note that when a rate of RSL rise is shown over a continental region, the number is to be interpreted as the rate of separation of the geoid and the surface of the solid earth.

Inspection of Plate 1 reveals a number of notable features, the most striking of which concerns the regions that were once ice covered and the areas immediately peripheral to them. In all ice-covered areas, sea level is currently falling at a rate near 1 cm yr^{-1}. Peripheral to these regions, sea level is predicted to be rising at

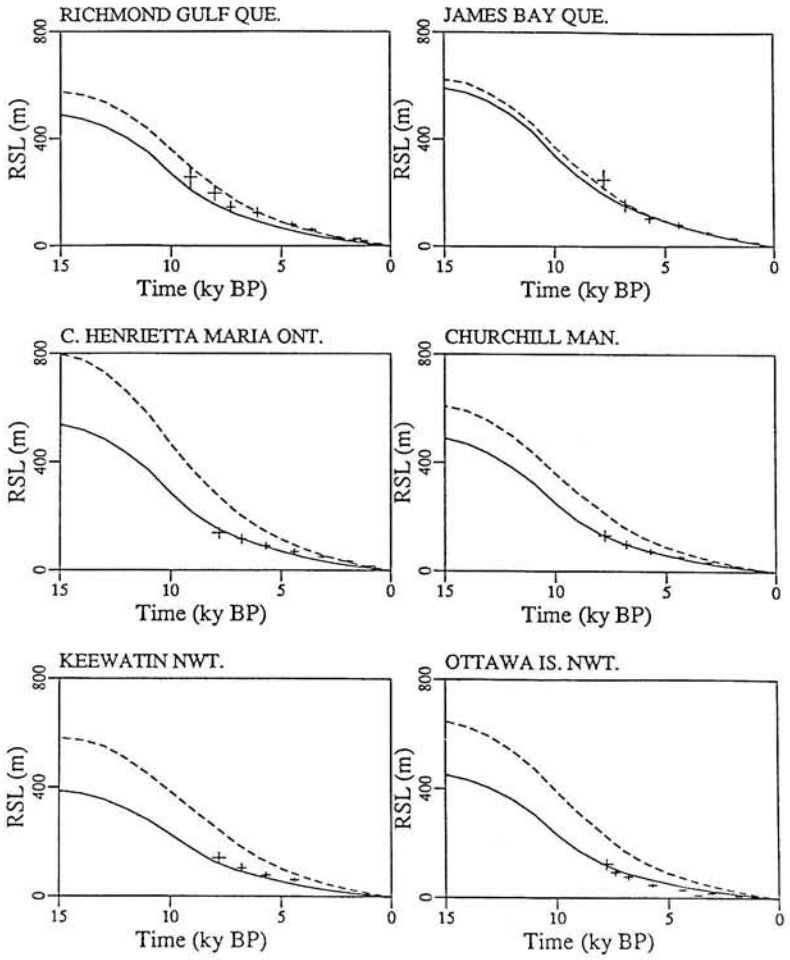

Fig. 3. Comparisons between observed and geophysically predicted RSL variations at six North American sites. The crosses denote the observed sea levels and their associated errors, while the solid and dashed curves denote two different theoretical predictions. The former is from the high-resolution isostatic adjustment model while the latter denote predictions from the lower resolution model of *Wu and Peltier* [1983].

present at maximum rates in excess of 2 mm yr^{-1}. Farther still from the glaciation centers the observed pattern is equally distinctive but of lower amplitude. Generally speaking, sea level along all continental coastlines in this "far-field" region is predicted to be falling at present at rates approaching 1 mm yr^{-1}. Oceanward of these continental coasts lies a "halo" within which sea level is essentially stagnant whereas in the ocean basin interiors sea level is again predicted to be falling at a rate less than 1 mm yr^{-1}. These patterns are all rather simply explicable in terms of the flow of material within the Earth's mantle that is forced by the changing surface ice and water loads. The fact that the isostatic adjustment signals are of the same magnitude in the regions peripheral to the ice sheet centers as the climate-related signal that may be recorded on the tide gage records very clearly suggests that the former contribution must be filtered from the tide gage records before the latter may be interpreted. In section 3 we will discuss the methodology that we have developed to achieve this goal.

DECONTAMINATION OF TIDE GAUGE RECORDS THROUGH REMOVAL OF THE "SECULAR" TREND DUE TO GLACIAL ISOSTATIC ADJUSTMENT

The tide gage records that we will analyze in this paper are those in the archive of the Permanent Service for Mean Sea Level (PSMSL) that is located at the Bidston Observatory, Birkenhead, Mersyside, United Kingdom. From this data base were obtained 554 records that had been verified at the Woods Hole Oceanographic Institute, among which there are 500 records of duration in excess of 10 years whose locations are shown on Figure 6. From this data set we removed a number of additional records either because they were from sites that were obviously tectonically active (e.g., Japan, Alaska), subsiding due to the influence of sedimentary loading (e.g., the Mississippi delta), or were "curiously" anomalous (e.g., Xiamen, China, where the rate of present-day sea level rise is apparently near 13.3 mm yr^{-1}). Of the remaining 470 records 12 of those of longest duration (all represented by annual means) are illustrated on Figure 7. Also shown superimposed upon each of the tide gage records is the secular sea level trend (dashed line) at each site that is predicted by the same geophysical model that was used to produce Plate 1. These dashed lines represent the contribution to the tide gage records due to the process of glacial isostatic adjustment. On Figure 8 we present a similar comparison of tide gage observation and isostatic adjustment prediction for Stockholm, Sweden, from which site an extremely long tide gage record is available [*Ekman*, 1988]. This record was compared to the considerably shorter version contained in the PSMSL data set, and for both records the linear regression estimate of the secular sea level trend is equal to

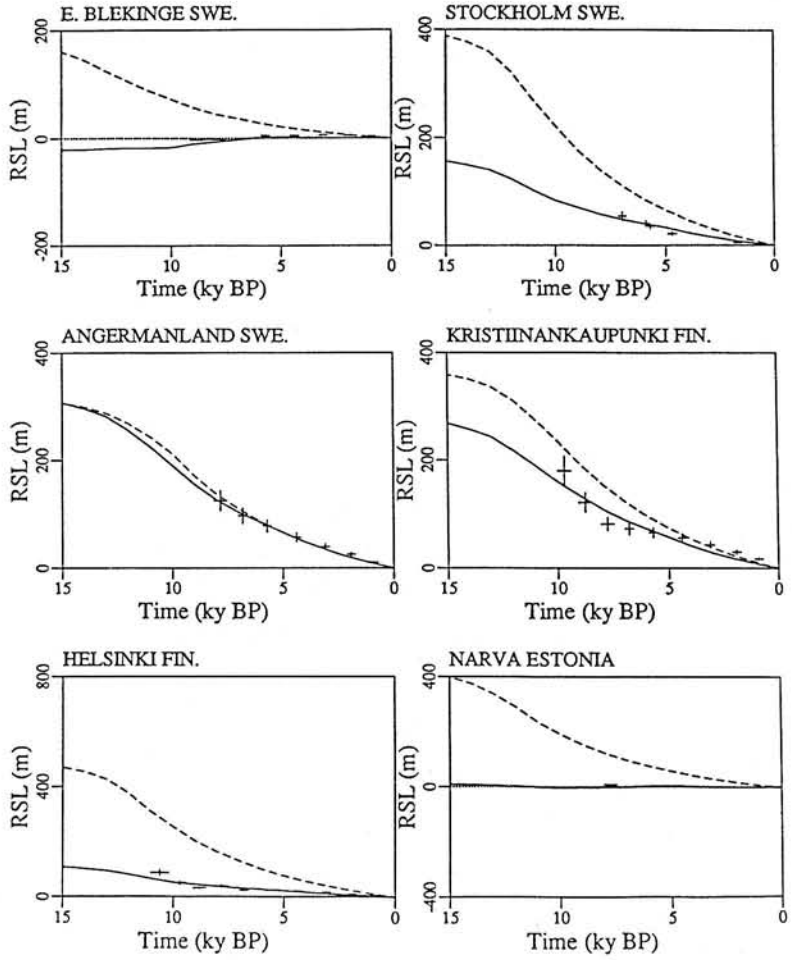

Fig. 4. Same as Figure 3 but for six European sites.

-4.1 mm yr^{-1}. Inspection of Figure 7 demonstrates furthermore that this trend is very accurately predicted by the glacial isostatic adjustment model and therefore is apparently entirely explicable in terms of this single physical process. Comparing this situation with that revealed at the other sites on Figure 7 shows that at eight of the 12 locations for which data are shown, the tide gage observed rate of relative sea level rise exceeds that predicted by the isostatic adjustment model whereas at the four remaining sites, three of which were ice covered (like Stockholm), the isostatic adjustment model quite accurately fits the tide gage measurement of the secular sea level trend.

For the purpose of the analyses that follow we have constructed a "reduced" set of tide gage data by simply subtracting the secular sea level trend predicted by the isostatic adjustment model from the annual mean tide gage signals to produce the set of time series on which the main conclusions of the following analyses will be based.

We have applied two different statistical estimation techniques to this reduced tide gage data set, namely, linear regression (LR) analysis and empirical orthogonal function (EOF) analysis. These two methods have different strengths and weaknesses and, as we shall see, provide useful cross-checks on the results obtained with either. Whereas EOF analysis requires that each of the tide gage records employed be continuous and of fixed duration, LR analysis may employ all of the records and is unaffected by the presence of gaps within them. On the other hand, LR analysis provides only a single linear trend per site and contains no internal mechanism for assessing the extent to which the data may be revealing a coherent spatial pattern such as we might expect to be characteristic of a signal associated with a global rise of sea level caused by greenhouse warming. A compilation of previous estimates of the secular sea level rise recorded on tide gauge data is presented in Table 1 along with brief commentary on the assumptions employed to do the analysis in each case. Inspection of the results in Table 1 shows that these previous estimates differ by as much as a factor of 3. These variations reflect variations in the length of the records employed for analysis, variations in the geographic locations of the stations utilized, and variations of statistical technique. In no previous case has a global analysis been performed within which the individual records have been corrected for isostatic adjustment. However, previous analysis of the tide gage data from stations in the U.S. network [*Peltier*, 1986] did show that the global analysis reported here would most probably deliver interesting results. We shall present the results of LR and EOF analysis in sequence in the following subsections.

3.1. *Results From Linear Regression Analysis*

The usual technique of linear regression estimates the secular rate of sea level rise, s, from each individual tide gauge record as

$$s = \frac{\sum t \cdot H - (\sum t)(\sum H)/n}{\sum t^2 - (\sum t)^2/n} \qquad (2)$$

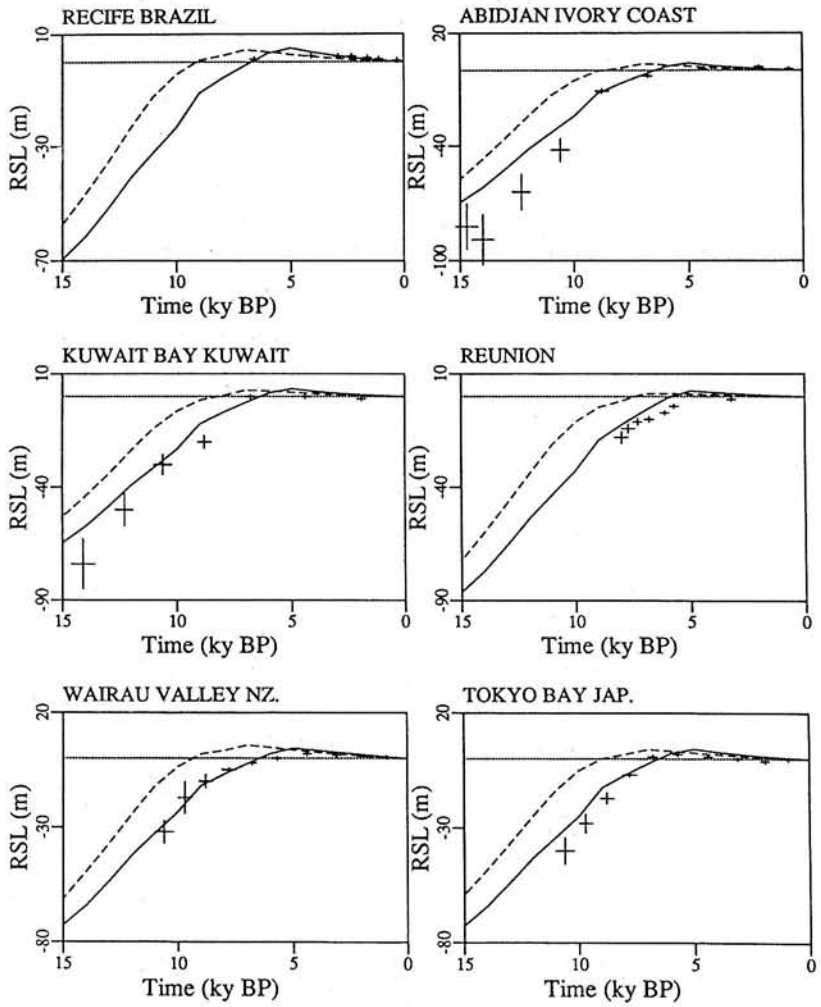

Fig. 5. Same as Figure 3 but for 6 far-field sites.

with t the individual sampling times, n the number of samples in the record, and H the annual mean sea level. The standard deviation of the data (σ) and the standard error (Δ) in the trend are similarly estimated as

$$\sigma = \frac{\sqrt{\sum H^2 - (\sum H)^2/n - s[\sum t \cdot H - (\sum H)(\sum H)/n]}}{n-2} \quad (3a)$$

$$\Delta = \frac{\sigma}{\sqrt{\sum t^2 - (\sum t)^2/n}} \quad (3b)$$

Because it was found that the average of the standard error in the trends was much smaller than the range of values obtained for the overall (global) trend due to changes either in the number of records analyzed or the type of analysis undertaken, we shall not comment further on the standard errors in what follows.

Inspection of Figure 6 reveals that the overwhelming number of tide gage sites are located in the northern hemisphere and are especially concentrated along the U.S. east coast and around the Baltic Sea. Because of the highly inhomogeneous geographic sampling of the ocean basins that the tide gage data provides, a simple site by site average of the secular sea level trends from the individual tide gages could not be expected to provide a reasonable statistical estimate of the globally averaged trend. In order to approximate more closely an equal-area average in order to overcome this sampling problem, we have therefore divided the global ocean into seven distinct regions within each of which the individual tide gage estimates are combined to generate a site-by-site average as an estimate for each region. The final equal-area average then weights the estimates for the individual areas according to the fraction of the total surface area that they individually represent to compute an estimate of the average rate of global sea level rise. The areas employed for this regionalization consist of the northwestern, northeastern, and southern Atlantic oceans, the Indian Ocean, and the northwestern, northeastern, and southern/central Pacific oceans whose fractional areas are respectively 8%, 8%, 15%, 20%, 12%, 10%, and 27% (the boundaries of these regions are shown on Figure 6).

LR analyses as described above were undertaken as a function of the minimum record length of the time series retained for analysis and for a reduced site-by-site average, for a reduced equal area average, and for an equal-area average of the raw data to which no isostatic adjustment correction was applied to "reduce" the signal. The results of these analyses are presented in Figure 9.

Plate 1. The present-day rate of RSL rise (fall) that should be recorded on a modern tide gage if the effect of glacial isostatic adjustment were the only contribution to present-day RSL change. The rates of RSL rise (fall) are in millimeters per year. Values shown over the continents represent the time rates of separation between the geoid and the surface of the solid earth.

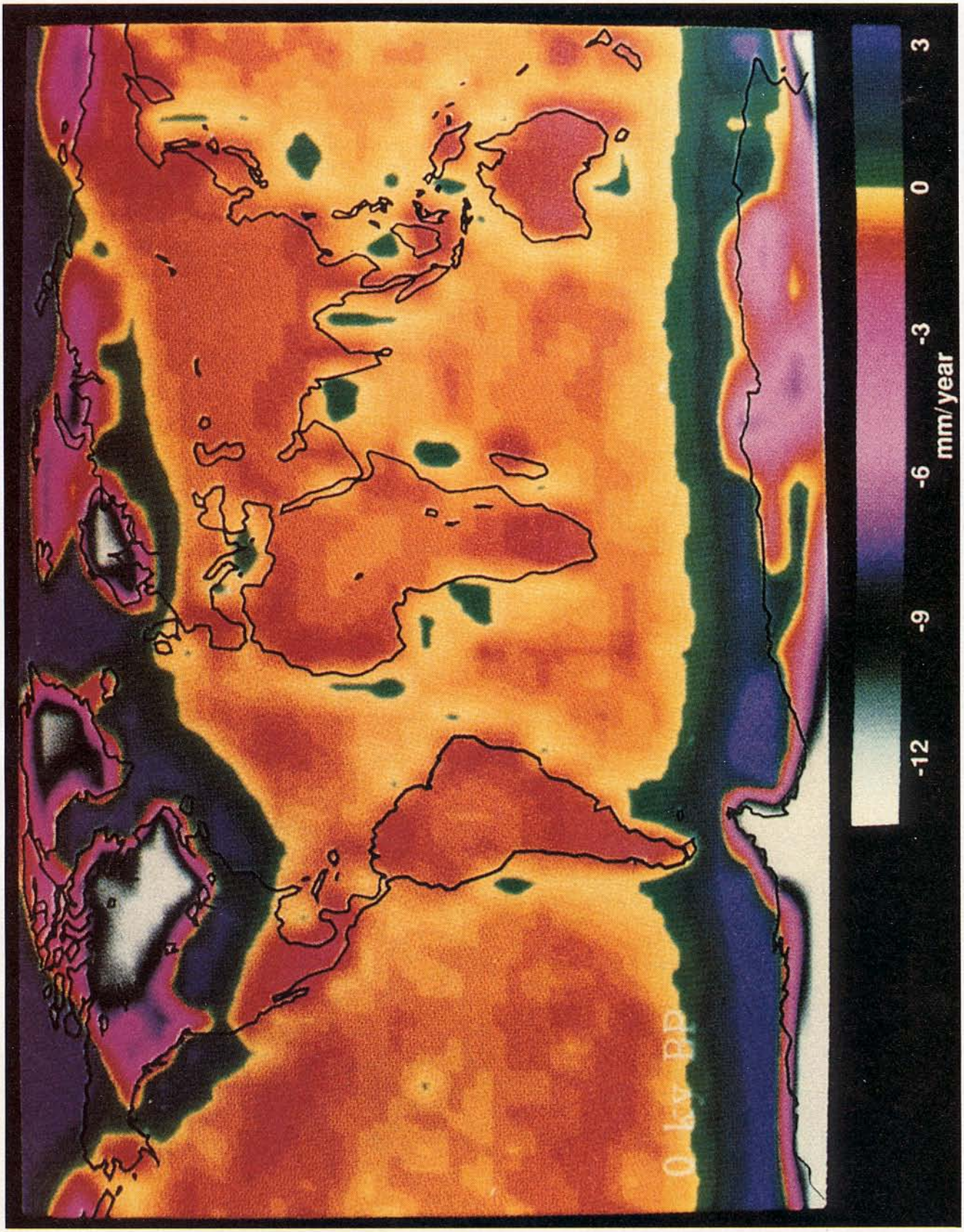
0 kyr BP
3
0
-3
-6
-9
-12
mm/year

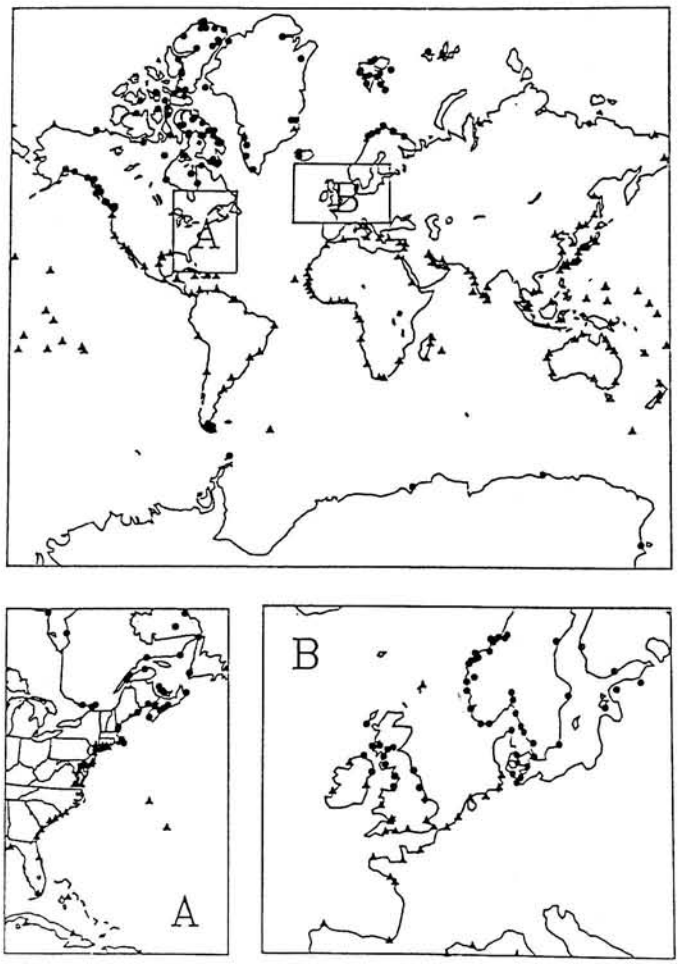

Fig. 6. Locations of the validated tide gages from which records are available that are of length greater than 10 year.
The data from these gages are archived with the Permanent Service for Mean Sea Level at Bidston, Merseyside, United Kingdom.

Inspection of Figure 9 shows that as the minimum record length threshold increases the number of tide gages available to form the estimate drops rapidly (dash-dotted line) such that only 179 stations are available at which the record length exceeds 30 years. With a threshold of 80 years, only 22 stations are available, and only three of these are located outside the northeastern Atlantic sector, making any equal-area average meaningless. Within the window from 30 to 80 years of minimum record duration the reduced site by site average (dotted curve) steadily decreases from 1.3 to 0.9 mm yr^{-1} while the reduced equal-area average increases from 1.6 mm yr^{-1} to 2.4 mm yr^{-1} at 55 years and then decreases sharply to 1.2 mm yr^{-1}. The equal-area average performed on the raw data (dashed curve) mimics the variation of the reduced equal-area average but delivers estimates of the secular rate of sea level rise that are lower than those delivered by equal area average of the reduced data by 0.4-0.5 mm yr^{-1}. Correcting the tide gage data for the influence of glacial isostatic adjustment therefore increases the inferred rate of secular sea level rise by a very substantial amount irrespective of the minimum record length employed in the statistical analysis. That this should be the case will be clear from Plate 1 on which we previously drew attention to the substantial rate at which sea level would be falling over much of the global ocean if the only influence were that of glacial isostatic adjustment.

The reason for the sharp fall of the estimate as the minimum record length increases beyond 60-70 years (see Figure 9) is that essentially all of the remaining long records are located in the Baltic Sea, and since this is a region of extremely rapid postglacial sea level fall due to ongoing postglacial rebound of the crust and since the tide gage records are swamped by this dominant signal, no residual signal is inferred to exist. The reason for the somewhat reduced estimates of the secular rate of rise of RSL that are obtained when the minimum record length is taken less than 30-40 years is that the time series are so short that an accurate estimate of the secular drift cannot be obtained. Between these two extremes of overly short and overly long threshholds for the minimum record length we see that something of a plateau develops between 40 and 50 years, and we propose to argue that on this plateau we achieve a "best" trade-off between the number of records employed to make the estimate and the spatial coaverage that these records provide. On this plateau we see that the reduced equal-area average estimate of the global rate of relative sea level rise is somewhat higher than 2.0 mm yr^{-1}. However, within the context of LR analysis there is no way in which we may properly judge the extent to which this inference of the globally averaged rate of sea level rise is meaningful. For this reason we turn to EOF analysis in order both to provide an independent statistical corroboration of the LR result and to extract additional independent information.

3.2. *Results From Empirical Orthogonal Function Analysis*

Unlike LR analysis, EOF analysis provides a means of assessing both the spatial and the temporal structures in the data and therefore a means of addressing the issue as to whether, for example, the temporal signal that we have inferred through LR analysis is spatially coherent. We will not rederive the basis of this method here, nor will we provide a detailed history of its use since it was first introduced [*Hotelling*, 1933; *Lorenz*, 1956], although it is important to realize that it has been previously employed for the same purpose to which it will be put here [*Barnett*, 1983; *Aubrey and Emery*, 1983] if on considerably smaller data sets. To apply the EOF methodology to the collection of time series that comprise the complete tide gage data set $M(\mathbf{x}, t)$ we have first removed the means of the individual series and reduced them each to unit variance by computing:

$$N(x,t) = \left[M(x,t) - \mu(x)\right]/\sigma(x) \tag{4}$$

in which $\mu(\mathbf{x})$ and $\sigma(\mathbf{x})$ are the individual mean heights and variances in the data of the station at location $\mathbf{x}$ respectively. The orthogonal function decomposition follows from the covariance matrices $\underline{\underline{A}} = \underline{\underline{N}}\,\underline{\underline{N}}^T/n_x\,n_t$ and $\underline{\underline{B}} = \underline{\underline{N}}^T\underline{\underline{N}}/n_x\,n_t$ where, n_x is the number of spatial points in the data set and n_t is the number of temporal points. If we define spatial and temporal eigenvectors $\mathbf{E}$ and $\mathbf{C}$ such that $(\underline{\underline{A}} - \lambda\,\underline{\underline{I}})\,\mathbf{E} = 0$ and $(\underline{\underline{B}} - \lambda\,\underline{\underline{I}})\,\mathbf{C} = 0$, then we may decompose $N(\mathbf{x}, t)$ as:

$$N(x,t) = \sum_{k=1}^{n} \left(\lambda_k n_x n_t\right)^{1/2} E_k(x)\; C_k(t) \tag{5}$$

which is the orthogonal function representation on which the EOF analysis is based. By construction the λ_k are the common eigenvalues of $\underline{\underline{A}}$ and $\underline{\underline{B}}$ while n is the smaller of n_x and n_t. Clearly, the dominant eigenvalue will provide a measure of the strength of the long-term rate of sea level rise, and only it and the next smaller eigenvalue will be explicitly analyzed here. To estimate the local rate of relative sea level rise for the station at location $\mathbf{x}$ we

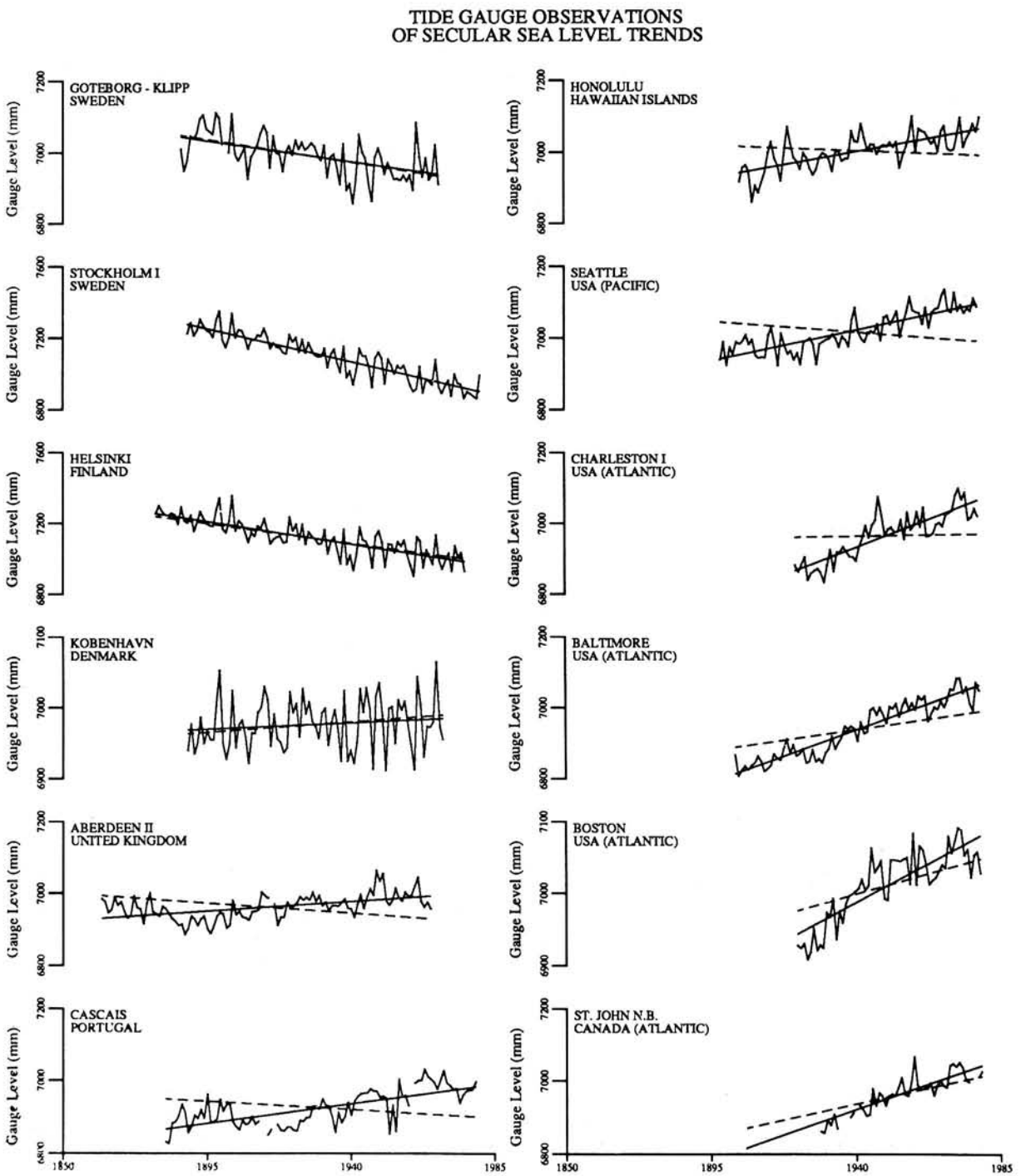

Fig. 7. Tide gage data from five North American, one Pacific Ocean and six European sites (solid curves) upon which are superimposed the best linear least squares fit to the data (solid lines) and the predicted secular sea level trend (dashed lines) based upon the same high resolution geophysical model used as basis for construction of the global map shown in Fig. 6.

simply multiply the least squares trend of $C_1(t)$ by $(\lambda_1 n_x n_t)^{1/2} E_1(x)$ and suppose that a global estimate is simply the site-by-site average of this product if the $E_1(x)$ are uniform.

Because EOF analysis is an "equal-time" technique which requires that each tide gage record be continuous and begin and end at the same date and since the complete data set does not fulfill these conditions, we are obliged to restrict analysis to a subset of the data, and for this purpose we have retained only those records for which essentially continuous series are available from 1920 through 1970. We are therefore choosing to work with records whose length equals the duration established by the preceding LR analysis as providing a best trade-off between length and spatial coverage. Where occasional gaps in these records were found to exist, these were filled by a linear least squares interpolate. No record was accepted if it was missing more than 10 years of data. On this basis we extracted 81 records that were amenable to EOF analysis from the complete PSMSL archive.

In order to appreciate better the impact which the isostatic adjustment correction has on the EOF estimate of the secular sea level trend we will first present the results delivered by the

TABLE 1. Estimates of the Present-Day Rate of Sea Level Rise

Reference	Estimate, mm yr^{-1}	Notes
Gutenberg [1941]	1.1	LR from 1806 to 1939
Hicks [1978]	1.5 ± 0.3	LR on US records only
Emery [1980]	3.0	included unstable records
Gornitz et al. [1982]	1.1 ± 0.1	thermal expansion of oceans
Aubrey and Emery [1983]	1.7	EOF on US records only
Barnett [1983]	1.5	EOF on 9 globally distributed records
This work	2.4 ± 0.9	EOF from 1920 to 1970 (isostatically corrected)

technique when it is employed to analyse the raw tide gage data. These results are shown on Figures 10*a* and 10*b* which show the primary and secondary spatial and temporal eigenvectors, respectively. On the basis of the associated primary and secondary eigenvalues these eigenvectors were found to account for 70% and 12% of the total variance with the remaining nonzero eigenvalues accounting for 18% of the variance. Inspecting the primary temporal eigenvector in Figure 10*b* (solid curve) demonstrates that there has been a consistent increase of sea level since 1920, while the secondary temporal eigenvector shows a slight decrease with extreme variability. The primary and secondary spatial eigenvectors are shown in Figure 10*a* and are the means through which EOF analysis allows us to judge the spatial coherence of the temporal patterns revealed by the associated temporal eigenvectors. To the extent that the primary spatial eigenvector is uniform, i.e., spatially invariant, the signal represented by the primary temporal eigenvector should be taken to represent a signal that is global in scale. Inspection of the primary spatial eigenvector in plate a of Figure 10 (solid curve), however, shows that this dominant temporal signal is highly inhomogeneous in space (sites are not named individually but rather are clustered into regions). The secondary spatial eigenfunction (dashed curve) indicates similar incoherence of the associated second-order spatial structure.

Although the first-order temporal structure that has been revealed by this analysis is highly inhomogeneous in space, the associated spatial structure nevertheless demonstrates that the inhomogeneity is quite strongly associated with the main centers of Pleistocene deglaciation and therefore suggests that filtering the data to remove the influence of this single process might substantially reduce the heterogeneity and thus give credence to the interpretation of the first-order temporal signal as being globally significant. For example, negative values of the first spatial eigenvector are almost without exception associated with sites around the Baltic Sea (which was ice covered at the maximum of Würm glaciation) and at which sea level is rapidly falling due to postglacial rebound of the crust. Since this signal is a factor of 5 stronger than the sea level rise observed elsewhere, it completely swamps the individual records in this region which are simply not long enough to allow any other source of variance to be discerned. Similarly, large positive values of the first spatial eigenvector are found in association with sites along the east coast of the continental United States which is a region of rapid present day postglacial submergence. The third characteristic segment of the first spatial eigenvector, for which moderately positive values of this parameter obtain, is made up of sites which are all located in regions remote from the main Pleistocene ice masses (the only exceptions to this rule being Wajima, Japan, and Astoria, Oregon, which have been kept in the data set but which are quite plausibly influenced by tectonic activity). Because these three regions are all defined in terms of their proximity to the perimeters of the main ice masses (i.e., Baltic Sea sites were within the perimeter of the Fennoscandian ice sheet, U.S. east coast sites were just outside the perimeter of the Laurentian ice sheet, and other sites were well removed from the ice sheet centers), we might expect to be able to eliminate the spatial heterogeneity by filtering the tide gage data so as to remove the isostatic adjustment contribution shown on Plate 1. The EOF methodology, through the first spatial eigenvector, will provide us with a quantitative measure of the extent to which this reduction of the data is able to improve the spatial coherence of the recovered signal. We will illustrate the impact of the filtering process on the interpretation by two further EOF analyses in which successively more stringent filtering will be applied.

To this end we first show in Figure 11 the results obtained when the complete reduced tide gage data set is subjected to the EOF analysis. Inspection of Figures 11*a* and 11*b* now shows that the original three distinct regions identified in the first spatial eigenvector have been reduced to two, consisting now of Baltic sites and all other locations. For all Baltic sites the magnitude of the first spatial eigenvector is very nearly zero, indicating that the first temporal eigenvector has essentially zero amplitude (i.e. no sea level rise is ongoing at these sites). At all other sites, however (again excluding Wajima, Japan, and Astoria, Oregon), the magnitude of the first spatial eigenvector fluctuates about a well-defined mean value near +0.55, indicating that at essentially all of these sites the linear sea level rise characteristic of the first temporal eigenvector is the main source of variance. In this analysis the primary and secondary eigenvalues now account for 50% and 22% of the variance, respectively, with the remaining nonzero eigenvalues accounting for 28%. In Figures 12*a* and 12*b*

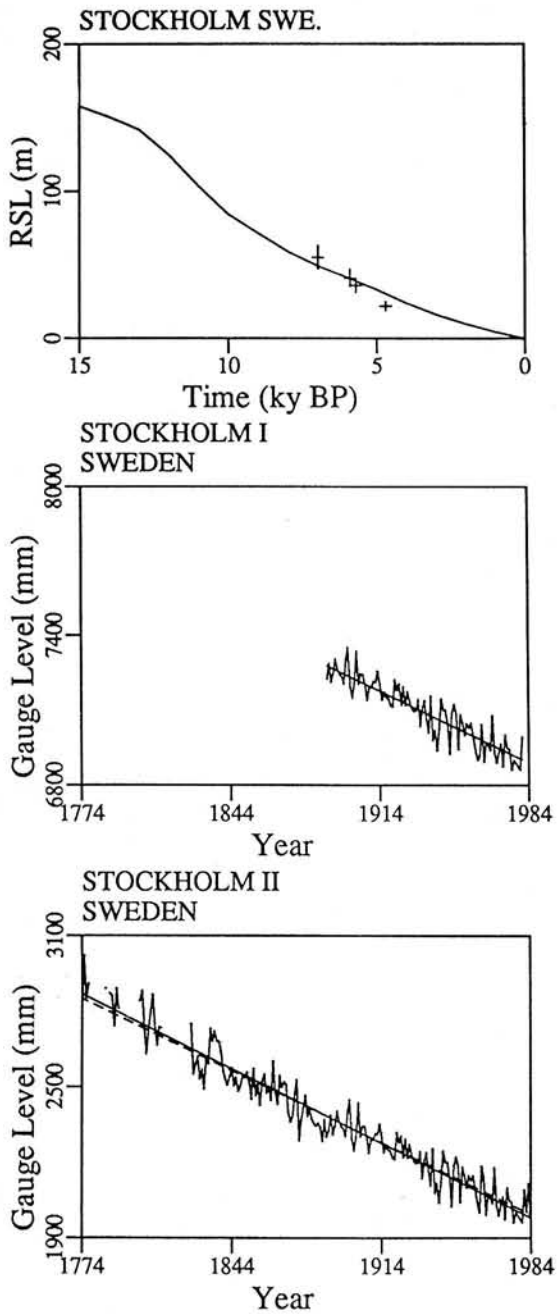

Fig. 8. Comparison of records from Stockholm, Sweden. The top figure compares the radiocarbon observations from Stockholm which extend back to about 7 ka with the geophysical predictions. The middle figure shows the PSMSL record for Stockholm compared to the geophysical prediction and the final plate presents this same comparison using the very long RSL record whose construction is discussed by *Ekman* [1988].

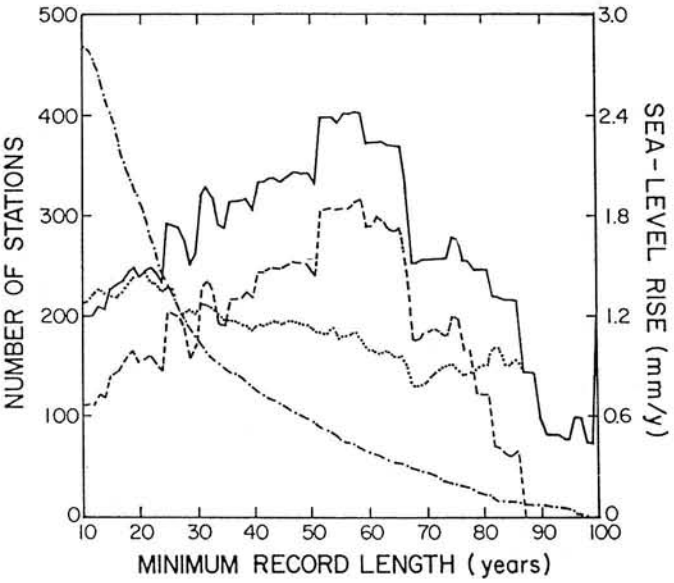

Fig. 9. Results for the global rate of relative sea level rise obtained from linear regression analysis. The dash-dotted curve depicts the manner in which the number of tide gage stations employed in the analysis decreases as the minimum record length accepted for analysis increases. The three individual estimates of the globally averaged rate of relative sea level rise for each choice of minimum record length are those based upon a direct site-by-site average (dotted curve), an equal-area average of the tide gage estimates uncorrected for the influence of glacial isostasy (dashed curve), and finally an equal-area average of the tide gage estimates adjusted so as to remove the effect of glacial isostatic disequilibrium (solid curve). The solid curve should provide the most accurate estimate of the globally average rate of present-day sea level rise.

we compare EOF and LR estimates of the secular sea level trend for the raw and isostatically reduced tide gage data, respectively. Inspection demonstrates the profound impact which the reduction process has upon the comparison. Although there is still considerable scatter that remains after the reduction procedure has been applied, it has been very sharply reduced with very few stations now indicating falling sea levels due to the inclusion of the Baltic sites at which the influence of postglacial rebound is dominant. Clearly, this effect has now been successfully removed.

The final set of analyses that we shall present in this section is based upon a data set constructed by eliminating all of the Baltic sites at which the RSL signal is known to be swamped by the crustal rebound induced by deglaciation. With these sites deleted (and also the supposed tectonically anomalous sites of Wajima, Japan, and Astoria, Oregon), we are left with a data set consisting of 40 time series, the locations of which are shown on Figure 13) that we consider to constitute the optimal set for inference of the globally averaged rate of sea level rise. The results of the EOF analysis on this data set are shown in Figure 14 and the EOF and LR estimates of the secular sea level trend are compared in Figure 15. In this EOF analysis the primary eigenvalue is now quite strongly dominant, representing 67% of the variance with the secondary eigenvalue representing only 7% of the variance and the rest (26%) carried by the remaining nonzero eigenvalues. Figure 14*a* shows that the dominant spatial eigenvector (solid curve) is now uniformally positive with much reduced variations about a well defined mean near 0.55. This is indicative of the fact that the dominant temporal eigenvector shown on Figure 14*b* (solid curve) is strongly characteristic of all sites in this data set and suggests a globally representative rate of sea level rise near 2.4 ± 0.9 mm yr^{-1}. The comparison of this EOF estimate of the secular sea level trend with the associated LR estimates on Figure 15 for the final 40 time series shows that a much tighter cluster is now defined by the data for the time period selected for analysis. A important issue nevertheless remains as to how sensitive this estimate of the global signal is to variations in the analysis procedure which test robustness of the result to plausible errors in the geophysical model that has been employed to "decontaminate" the tide gage data. This is the subject of the following and penultimate section of the present paper.

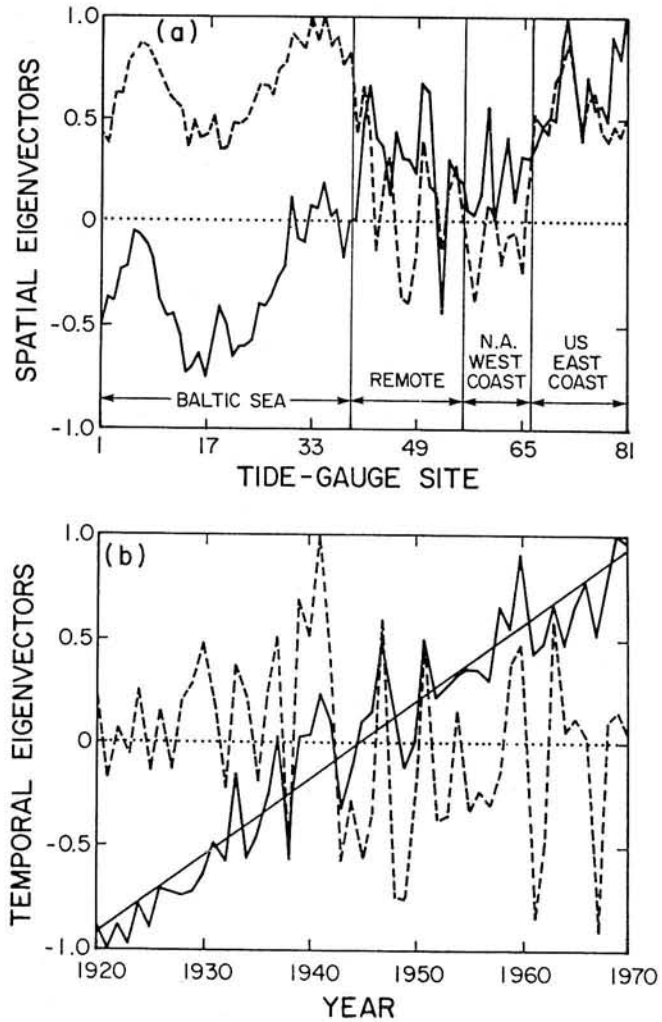

Fig. 10. Results for the global rate of sea level rise obtained from empirical orthogonal function analysis of the raw tide gage data. Only the two dominant spatial and temporal eigenvectors are explicitly shown in Figures 10*a* and 10*b*, respectively. (*a*) The dominant spatial eigenvector (solid curve) and secondary spatial eigenvector (dashed curve). (*b*) The dominant temporal eigenvector (solid curve) is superimposed upon the best least squares linear trend fitted to these data. The secondary temporal eigenvector is shown as the highly irregular dashed line.

SENSITIVITY OF THE ESTIMATED GLOBAL RATE OF RSL RISE TO VARIATIONS IN THE ANALYSIS PROCEDURE

In order to investigate this final issue we have performed a number of analyses in addition to those discussed above but using the same procedures. These analyses are of two different types: one designed to investigate the sensitivity of the final result to plausible variations of the geophysical model that is employed to filter the isostatic adjustment signal from the tide gage data, and the other to investigate the sensitivity of the result to the time period over which the analysis is performed and the length of the time series employed.

The results of the first of these additional sets of analyses are summarized succinctly in Table 2. For the most part Table 2 is self-explanatory but a number of inferences that follow from the numerical data in Table 2 do warrant individual mention. The first column of Table 2 describes the characteristics of the geophysical model that are being varied in the sensitivity tests, the results of which are shown in the columns for the model corresponding to the entries in each row. In the first column the terms uncorrected and standard imply that the tide gage data are uncorrected for the influence of glacial isostasy or are corrected with the standard geophysical model employed for all of the results presented in section 5. The section of Table 2 that provides results for the 81 gauges with 50 year records includes the records from Baltic sites in the analysis, while in the section labeled "40 Tide Gage Records", all of the data from the Baltic locations are deleted.

The variation upon the standard analysis procedure represented by the data in the row labeled RSL is especially important. For these analyses we used the radiocarbon records themselves to correct the tide gage data rather than the geophysical model wherever a sufficiently proximate ^{14}C- controlled long timescale RSL history was available. This alternate method of correcting the data was considered practicable at 28 of the 40 non-Baltic tide gage sites. From Table 2 it will be noted that employing this alternative method of correcting the data actually reduces the estimate of the global rate of RSL rise somewhat, from 2.4 ± 0.9 to 2.1 ± 0.8 mm yr^{-1}. Most interesting in this initial set of geophysical comparisons, however, is the comparison between the result of the analysis of the uncorrected data and the result

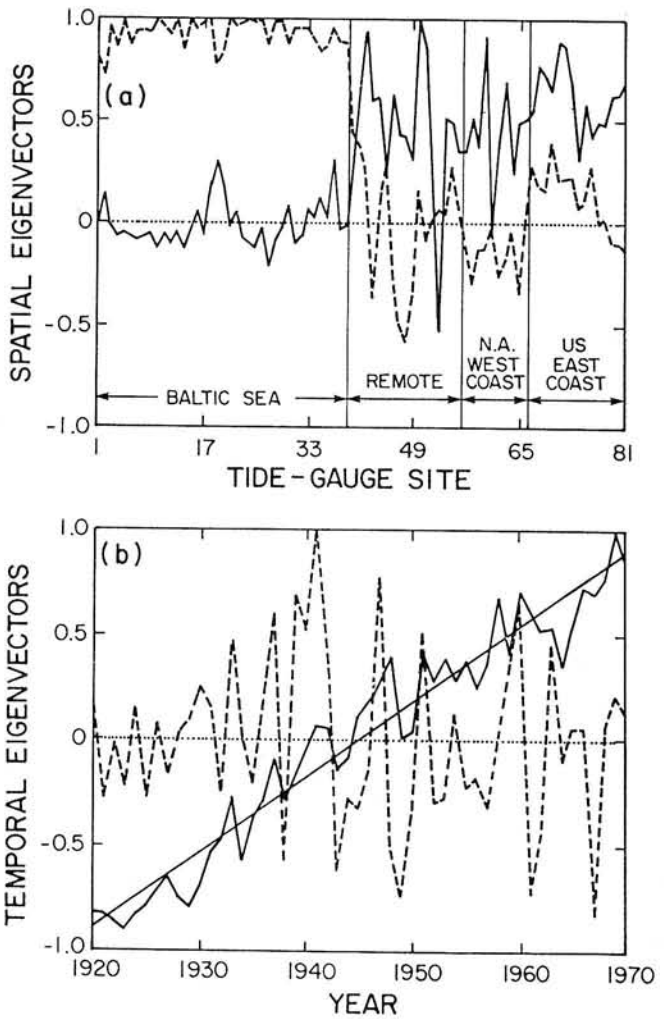

Fig. 11. Same as Figure 10 but for the "reduced" tide gage data set constructed by subtracting the geophysically predicted isostatic adjustment signal from the raw sea level trend determined by the tide gage data at each site.

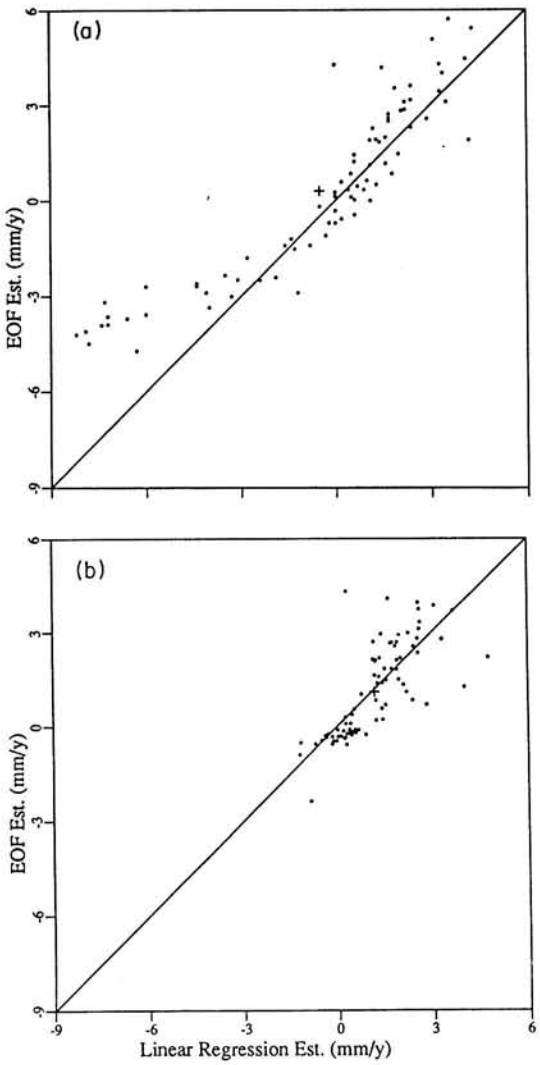

Fig. 12. Comparison between EOF and LR determinations of the secular sea level trend at each of the 81 sites. (*a*) Comparison for the analyses based upon the raw tide gage data. (*b*) Same comparison for the analyses based on the tide gage data after application of the isostatic adjustment correction.

obtained after reduction with the standard geophysical model. The former procedure (EOF) gives 2.2 ± 1.4 mm yr^{-1}, whereas the latter gives 2.4 ± 0.9 mm yr^{-1}. It might be seen as surprising, given our previous commentary, that the raw data and the isostatically corrected data deliver such modestly discrepent results.There are two points to be made about this, however. First, one should note the marked increase in the standard deviation on the estimate from the raw data. Second, this implies that the isostatic filtering procedure is acting such as to lower the estimates at some sites which are spuriously high and to decrease other estimates that are spuriously low. Reference to the individual time series demonstrates that about half of the raw series, those along the east coast of the continental United States, are anomalously high because they are located on the collapsing forebulge of the Laurentide ice sheet. Likewise most of the remaining sites are anomalously low because they lie along continental coastlines in the far field where tide gages record anomalously low rates of present-day relative sea level rise due to the tilting effect along such coastlines caused by the offshore water load that is applied to the ocean basins by ice sheet disintegration.

The remaining rows in Table 2 document the impact upon the global estimate of RSL rise of modifications to the radial viscoelastic structure of the geophysical model. With the elastic structure fixed to that of 1066B we first vary lithospheric thickness. With lithospheric thickness fixed we then vary lower mantle viscosity. Penultimately we insert a low viscosity channel of 100 km thickness (LVZ) into the standard model immediately below the lithosphere of standard thickness 120 km, and then finally we replace the 1066B elastic structure with the PREM structure of *Dziewonski and Anderson* [1981].

Inspection of these remaining entries in Table 2 reveals the following facts. First, we note that the lower the lithospheric thickness the lower the global estimate of the rate of RSL rise. This is because the diminution of the contribution from U.S. east coast peripheral bulge sites (the amplitude of the bulge is enhanced by the decreased lithospheric thickness) is a stronger effect than the enhancement of the contribution at far field sites (due to the increase of the effect of tilting of the crust due to the offshore water load; see *Peltier* [1988*a*] for examples of this effect). The result for a lithospheric thickness labeled "mixed" employs the geophysical model with 295 km lithospheric thickness to reduce the tide gage data from U.S. east coast sites and the standard

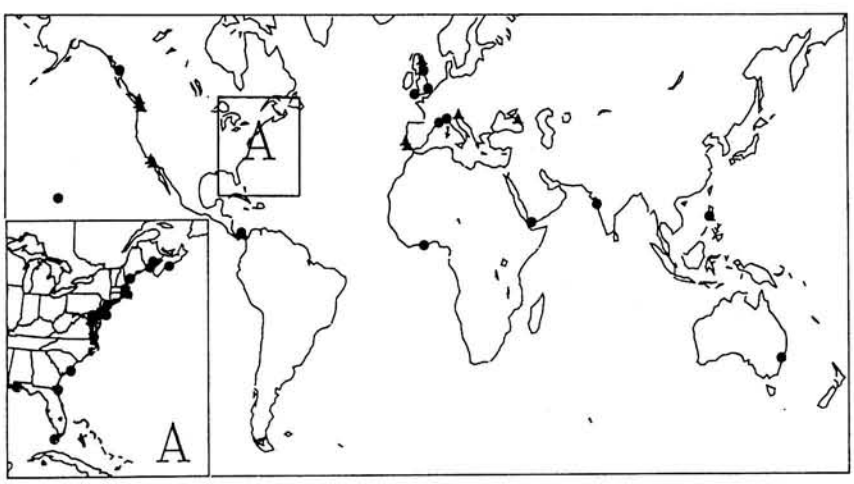

Fig. 13. The location of the 40 tide gauge sites. The dots represent locations which have nearly long-term RSL data, whereas those locations denoted by triangles do not.

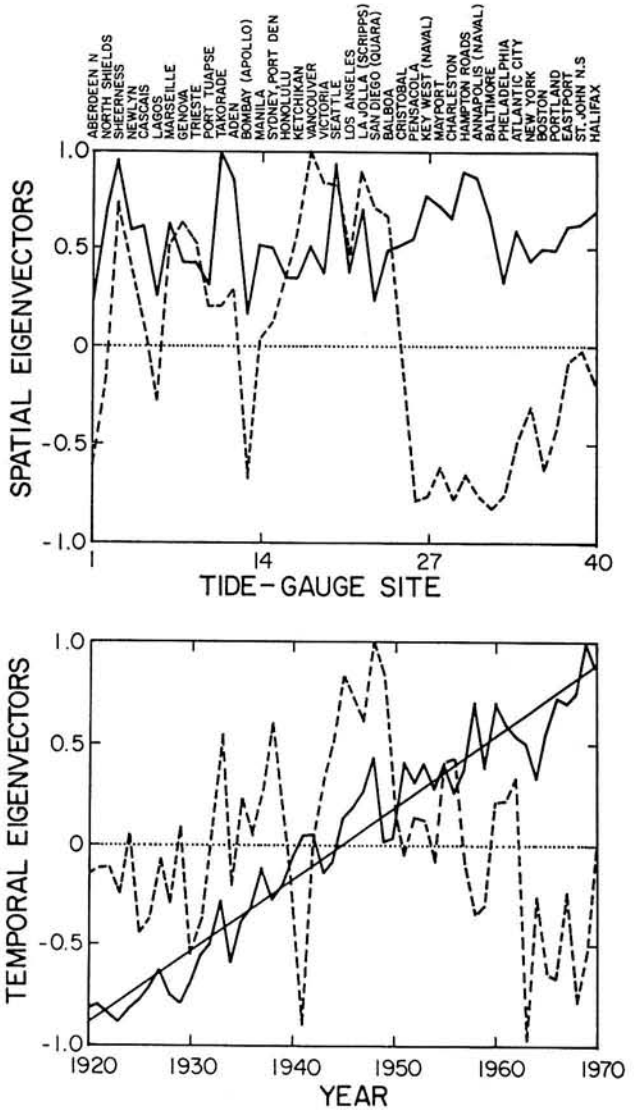

Fig. 14. Same as for Figure 6 but for the reduced data from the 40 tide gage stations with records of 50 years' duration that remain once the Baltic data are eliminated. Two additional records (Wajima, Japan, and Astoria, Oregon) have also been eliminated.

model with lithospheric thickness of 120 km to reduce the data from all other gages. This result, which should in fact be the most accurate in the set, as *Peltier* [1985] has shown the ^{14}C data from the U.S. east coast to require such increased lithospheric thickness, increases the global estimate to 2.8 ± 1.1 mm yr^{-1}. Although lithospheric thickness changes do systematically impact the RSL estimate, the same is clearly not the case for lower mantle viscosity as inspection of the following rows in Table 2 demonstrates.

Of the final two sensitivity analyses for which results are displayed in Table 2, those for the models denoted LVZ are clearly the most dramatic. This innovation is seen to reduce the inferred global rate of RSL rise to 1.4 mm yr^{-1}. However such models are incompatible with the ^{14}C data from North America, and therefore this model is the least accurate filter of the isostatic adjustment effect employed in any of the sensitivity tests discussed here. The final geophysical model employed to reduce the data, that labeled PREM in Table 2, has a viscous structure identical to that of the standard model but PREM elastic structure. This has essentially no influence on the estimate (a minor increase to 2.5 mm yr^{-1}).

The final general class of sensitivity tests that we will discuss here is in many ways the most important because it in principal provides the means by which the mechanism of the present-day rate of RSL rise may be best assessed. This concerns the dependence of the inferred rate upon the time interval over which the average is performed and the length of the time series employed to compute the average. If we could convincingly show, for example, that the global rate of RSL rise was an increasing function of time, then a more plausible connection might be made between the greenhouse effect and the observed signal since the rate of increase of mean surface temperature due to this cause has presumably been accelerating with the increase in the atmospheric concentration of CO_2 and other radiatively active trace gases. The results of all of these analyses are summarized in Table 3 in which we first illustrate the variation of the inferred rate of RSL rise with time based upon the use of time series of length 51 years and then the variation of the estimate up to 1970 using sets of time series of decreasing duration. Noticeable by inspection of the entries in Table 3 is first the fact that from the early 1900's until the present the rate of RSL rise does indeed seem to have increased with time, at least until the 50-year period 1930-1980 over which the rate fell from the rate of 2.4 ± 0.9 mm yr^{-1} characteristic of the period 1920-1970 to the rate of 1.5 ± 0.6 mm yr^{-1}. It will be noted from Table 3, however, that the number of stations from which data were available also fell from the maximum of 40 non-Baltic sites employed in the standard analysis to 33. Although this does significantly degrade the sample, the result does suggest that the result from the analysis of this sample is significantly determined by a minority (18%) of the time series and therefore gives real cause for concern as to whether the higher rate may be construed as a truly globally representative estimate. Further analysis will be required to assess adequately these differences, but we must certainly conclude on the basis of them that no statistically

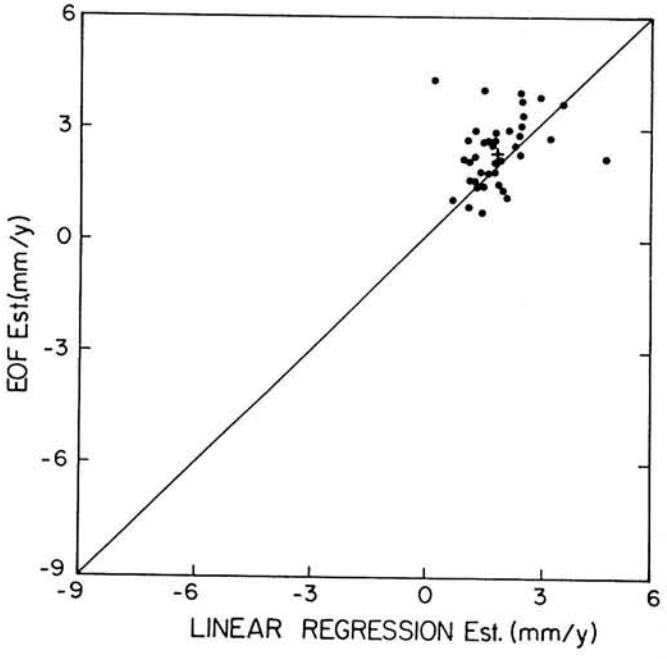

Fig. 15. Comparison between EOF and LR determination of the secular RSL trend at the 40 sites selected as the optimal set for the global inference. A reasonably tight cluster is delivered by the two types of analysis.

TABLE 3. Time Dependency of the Tide Gage Records

Window Width, years	Start Year	End Year	Number of Records Available	First Eigen-value %	Second Eigen-value %	Mean of First Spatial E. Vect.	SD of First Spatial E. Vect.	LR Estimated of SL Rise, mm/yr	SD of LR Estimated mm/yr	EOF Estimated of Sea Level Rise, mm/yr)	SD of EOF Estimated mm/yr	Avg. Scat. Dist. mm/yr
						Fixed Window Width						
51	1890	1940	11	66	8	.31	.30	1.6	1.5	0.7	0.7	.467
51	1900	1950	20	52	9	.54	.28	1.6	0.9	1.2	0.6	.235
51	1910	1960	27	57	8	.58	.26	1.8	0.8	1.4	0.6	.191
51	1920	1970	40	67	7	.56	.21	2.3	0.8	2.4	0.9	.192
51	1930	1980	33	58	10	.57	.22	2.0	1.1	1.5	0.6	.215
						Variable Window Width						
71	1900	1970	13	68	7	.58	.23	1.9	0.8	1.2	0.5	.250
66	1905	1970	17	66	6	.58	.25	1.9	0.8	1.2	0.5	.224
61	1910	1970	24	67	5	.58	.24	1.9	0.8	1.5	0.6	.196
56	1915	1970	29	65	7	.51	.22	2.1	0.8	1.7	0.7	.197
51	1920	1970	40	67	7	.56	.21	2.3	0.8	2.4	0.9	.192
46	1925	1970	52	65	7	.46	.23	2.2	1.0	2.3	1.1	.210
41	1930	1970	66	56	10	.43	.25	1.9	1.1	1.9	1.1	.192
36	1935	1970	82	46	11	.30	.22	1.6	1.5	1.4	1.0	.200

All tide gage records have been reduced using the standard model.

TABLE 2. Statistical Analysis of Tide Gage Records

Model	Density/ Elastic Model	Lithos-phere Thickness, km	Lower Mantle Viscosity (Pa s)	First Eigen-value, (%)	Second Eigen-value (%)	Mean of First Spatial E. Vec.	SD of First Spatial E. Vect.	LR Estimated of SL Rise, mm/yr	SD of LR Estimated mm/yr	EOF Estimated of SL Rise mm/y	SD of EOF Estimated mm/yr	Average Scat. Dist. mm/yr
						81 Tide Gage Records						
Uncorrected	-----	---	-----	70	12	0.05	0.45	-0.5	3.8	0.4	2.9	0.527
Standard	1066B	120	$2x10^{21}$	50	22	0.26	0.34	1.5	1.2	1.1	1.5	0.230
						40 Tide Gage Records						
Uncorrected	-----	---	-----	74	5	0.42	0.26	2.4	1.3	2.2	1.4	0.293
Standard	1066B	120	$2x10^{21}$	67	7	0.56	0.21	2.3	0.8	2.4	0.9	0.192
RSL**	1066B	120	$2x10^{21}$	65	7	0.51	0.20	2.2	0.8	2.1	0.8	0.180
Various		71		68	7	0.52	0.23	2.3	0.9	2.3	1.0	0.214
lithospheric	1066B	196	$2x10^{21}$	69	6	0.56	0.24	2.3	0.9	2.5	1.1	0.217
thicknesses		245		71	6	0.56	0.26	2.4	0.9	2.6	1.2	0.241
		Mixed*		71	6	0.59	0.24	2.5	0.8	2.8	1.1	0.221
Various			$1x10^{21}$	69	7	0.49	0.21	2.3	1.0	2.2	1.0	0.214
lower	1066B	120	$4x10^{21}$	68	7	0.55	0.22	2.3	0.8	2.4	1.0	0.196
mantle			$1x10^{22}$	70	7	0.49	0.23	2.4	0.9	2.2	1.0	0.212
viscosities			$1x10^{24}$	68	7	0.51	0.21	2.3	0.9	2.2	0.9	0.200
LVZ***	1066B	120	$2x10^{21}$	61	9	0.39	0.23	1.9	1.0	1.4	0.8	0.209
PREM	PREM	120	$2x10^{21}$	68	7	0.57	0.22	2.3	0.8	2.5	1.0	0.199

All tide gage records have been analyzed between 1920 and 1970.

*Eastern North American sites reduced using 245-km model; all other sites reduced using 120-km model

**28 of the 40 sites reduced using long-term RSL data; remaining 12 sites reduced using Std. model.

***All models have an upper mantle (above 670 km) viscosity of $1x10^{21}$ Pa s except the low viscosity zone model which has a viscosity of $1x10^{20}$ Pa s in the uppermost 100 km and $1x10^{21}$ Pa s below.

significant acceleration in the global rate of RSL rise is detectable in the set that we have analyzed when the data are isostatically corrected. The final section of Table 3 also illustrates an important further point, namely that the rate delivered by the standard analysis procedure using records of 50 years duration from 1920-1970 is the highest rate obtained for any period X-1970 whether X is earlier than 1920 in which case one has fewer records to analyze or whether X is later than 1920 in which case one has more records to analyze. This casts some further doubt upon the extent to which we should be prepared to accept the 2.4 $\pm$ 0.9 mm yr^{-1} standard estimate as reliable.

CONCLUSIONS

In our view the main point that has been established by the preceding analyses is that modern tide gage measurements of secular sea level trends are strongly influenced by the ongoing process of glacial isostatic adjustment. This influence is pervasive. In regions that were ice covered at the last glacial maximum it is so dominant an effect that no additional signal may be unambiguously extracted from the records. In regions peripheral to the main centres of glaciation such as the east coast of the continental United States the signal is of the same order as the residual signal that could be related to climate warming, and being of the same sign as this signal biases it upward by as much as 2 mm yr^{-1}. Along all continental coastlines in the "far field" of the ice sheets the tilting of the land induced by the offshore water load produced by deglaciation [e.g., *Clark et al.*, 1978] is responsible for the currently falling sea levels that are observed on ^{14}C records of RSL change from such sites. This effect clearly biases the climate related RSL signal to lower values.

When this geographically heterogeneous isostatic adjustment bias is removed from tide gage records of secular sea level change, it is found that the global residual signal so revealed is considerably more coherent geographically than was that characterized by the unfiltered data. This residual signal is therefore more plausibly associated with global climate warming. Our best estimate of the present-day global rate of RSL rise is 2.4 $\pm$ 0.9 mm yr^{-1} which is considerably higher than past estimates based upon analyses of data that were not corrected for the influence of glacial isostatic adjustment. It should be noted, however, that this estimate has been shown to be extremely sensitive to relatively modest alterations of the analysis procedure. Further analyses of the type reported here, in which other quantifiable influences such as that associated with slow variations in the strength of the onshore component of wind stress are removed from the records, are clearly in order as is effort to improve the quality of the data base itself.

REFERENCES

Aubrey, D.G., and K.O. Emery, Eigenanalysis of recent United States sea level, *Cont. Shelf Res.*, *2*, 21-33, 1983.

Aubrey, D.G., and K.O. Emery, Recent global sea levels and land levels, paper presented at the International Workshop on Climate Change, Sea Level, Severe Tropical Storms and Associated Impacts, United Nations Environment Programme, the Commission of the European Communities and the U.S. Environmental Protection Agency, Norwich, England, June 1988.

Barnett, T.P., Recent changes in sea level and their possible causes, *Clim. Change*, *5*, 15-38, 1983.

Barnett, T.P., The estimation of "Global" sea level change: A problem of uniqueness, *J. Geophys. Res.*, *89*, 7980-7988, 1984.

Clark, J.A., W.E. Farrell and W.R. Peltier, Global changes in postglacial sea level: A numerical calculation, *Quat. Res.*, *9*, 265-287, 1978.

Dziewonski, A.M. and D.L. Anderson, Preliminary reference Earth model, *Phys. Earth. Planet. Inter.*, *25*, 279-356, 1981.

Ekman, M., The world's longest continued series of sea level observations, *Pure Appl. Geophys.*, *127*, 73-77, 1988.

Emery, K.O., Relative sea levels from the tide gauge records, *Proc. Natl. Acad. Sci.*, *77*, 6968-6972, 1980.

Fairbridge, R.W., and O.A. Krebs, Jr., Sea level and the Southern Oscillation, *Geophys. J. R. Astron. Soc.*, *6*, 532-545, 1962.

Gilbert, F., and A.M. Dziewonski, An application of normal mode theory to retrieval of structural parameters and source mechanisms from seismic spectra, *Philas. Trans. R. Soc. London, Ser. A*, *278*, 187-269, 1974.

Gornitz, V., S. Lebedeff, and J. Hansen, Global sea level trend in the past century, *Science*, *215*, 1611-1614, 1982.

Gutenberg, B., Changes in sea level, postglacial uplift, and mobility of the Earth's interior, *Geol. Soc. Am. Bull.*, *52*, 721-772, 1941.

Hicks, S.D., An average geopotential sea level series for the United States, *J. Geophys. Res.*, *83*, 1377-1379, 1978.

Hotelling, H., Analysis of a complex of statistical variables into principle components, *J. Educ. Psych.*, *24*, 417-441, 1933.

Lorenz, E.N., Empirical orthogonal functions and statistical weather predictions, *Sci. Rep. 1*, 49 pp., Stat. Forecasting Proj., Dep. of Meteorol., Mass. Inst. of Technol., Cambridge, 1956.

Meier, M.F., Contribution of small glaciers to global sea level, *Science*, *226*, 1418-1421, 1984.

Mitrovica, J.X., and Peltier, W.R., Pleistocene deglaciation and the global gravity field, *J. Geophys. Res.*, *94*, 13,651-13,671, 1989.

Mitrovica, J.X., and W.R. Peltier, A formalism for the objective inversion of glacial isostatic adjustment data, *Geophys. J.*, in press.

Peltier, W.R., The impulse response of a Maxwell Earth, *Rev. Geophys.*, *12*, 649-669, 1974.

Peltier, W.R., Glacial-isostatic adjustment, II, The inverse problem, *Geophys. J.R. Astron. Soc.*, *46*, 669-706, 1976.

Peltier, W.R., Ice age geodynamics, *Annu. Rev. Earth Planet. Sci.*, *9*, 199-225, 1981.

Peltier, W.R., Dynamics of the ice age Earth, *Adv. Geophys.*, *24*, 1-146, 1982.

Peltier, W.R., The rheology of the planetary interior, *Rheology*, *28(b)*, 665-697, 1984.

Peltier, W.R., Climatic implications of isostatic adjustment constraints on current variations of eustatic sea level, in *Glaciers, Ice Sheets and Sea Level: Effect of a CO_2-Induced Climatic Change*, 92-103, National Academy of Science Press, Washington, D.C., 1985.

Peltier, W.R., Deglaciation-induced vertical motion of the North American continent and transient lower mantle rheology, *J. Geophys. Res.*, *91*, 9099-9123, 1986.

Peltier, W.R., Global sea level and Earth rotation, *Science*, *240*, 895-901, 1988*a*.

Peltier, W.R., Lithospheric thickness, Antarctic deglaciation history, and ocean basin discretization effects in a global model of postglacial sea level change: A summary of some sources of nonuniqueness, *Quat. Res.*, *29*, 93-112, 1988*b*.

Peltier, W.R., and J.T. Andrews, Glacial-isostatic adjustment, I, The forward problem, *Geophys. J. R. Astron. Soc.*, *46*, 605-646, 1976.

Peltier, W.R., and A.M. Tushingham, Global Sea Level rise and the greenhouse effect: Might they be connected, *Science*, *244*, 806-810, 1989

Peltier, W.R., and P. Wu, Mantle phase transitions and the free air gravity anomalies over Fennoscandia and Laurentia, *Geophys. Res. Lett.*, *9*, 731-734, 1982.

Peltier, W.R., W.E. Farrell, and J.A. Clark, Glacial isostasy and relative sea level: A global finite element model, *Tectonophysics*, *50*, 81-110, 1978.

Roemmich, D., Sea level and the thermal variability of the ocean, in *Glaciers, Ice Sheets and Sea Level: Effect of a Co_2-Induced Climate Change*, pp. 104-115, National Academy of Science Press, Washington, D.C., 1985.

Roemmich, D. and C. Wunsch, Apparent changes in the climatic state of the deep North Atlantic Ocean, *Nature*, *307*, 447-450, 1984.

Tushingham, A.M., and W.R. Peltier, ICE-3G: A new global model of late

pleistocene deglaciation based upon geophysical predictions of post-glacial relative sea level change, *J. Geophys. Res.*, in press, 1990*a*.

Tushingham, A.M. and W.R. Peltier, Validation of the ICE-3G model of Würm-Wisconsin deglaciation using a global data base of relative sea level histories, *J. Geophys. Res.*, in press, 1990b.

Wu, P., and W.R. Peltier, Viscous gravitational relaxation, *Geophys. J.R. Astron. Soc.*, *70*, 435-486, 1982.

Wu, P., and W.R. Peltier, Glacial isostatic adjustment and the free air gravity anomaly as a constraint on deep mantle viscosity, *Geophys. J. R. Astron. Soc.*, *74*, 377-450, 1983.

Wu, P., and W.R. Peltier, Pleistocene deglaciation and the Earth's rotation: A new analysis, *Geophys. J. R. Astron. Soc.*, *76*, 753-791, 1984.

W.R. Peltier and A.M. Tushingham, Department of Physics, University of Toronto, Toronto, Ontario, Canada M5S 1A7

(Reveived October 19, 1989;
revised May 8, 1990;
accepted June 22, 1990.)